Computational Modeling of the Structure-Function Relationship in Human Placental Terminal Villi

R. Plitman Mayo[a,b], J. Olsthoorn[c], D. S. Charnock-Jones[b,d], G. J. Burton[b], M. L. Oyen[a,b,*]

[a]*Nanoscience Centre, Department of Engineering, University of Cambridge, Cambridge, CB3 0FF, UK*
[b]*Centre for Trophoblast Research (CTR), Department of Physiology, Development and Neuroscience, University of Cambridge, Cambridge, CB2 3EG, UK*
[c]*Department of Applied Mathematics and Theoretical Physics, University of Cambridge, Cambridge, CB3 0WA*
[d]*Department of Obstetrics & Gynaecology, University of Cambridge, Cambridge, CB2 0SW, UK*

Abstract

Placental oxygen transport takes place at the final branches of the villous tree and is dictated by the relative arrangement of the maternal and fetal circulations. Modeling techniques have failed to accurately assess the structure-function relationship in the terminal villi due to the geometrical complexity. Three-dimensional blood flow and oxygen transport was modeled in four terminal villi reconstructed from confocal image stacks. The blood flow was analyzed along the center lines of capillary segments and the effect of the variability in capillary diameter, tortuosity and branching was investigated. Additionally, a validation study was performed to corroborate the simulation results. The results show how capillary variations impact motion of the fetal blood, and how their bends and dilatations can decelerate the flow by up to 80%. Vortical flow is also demonstrated not to develop in the fetal capillaries. The different geometries are shown to dictate the transport of gases with differences of over 100% in the oxygen flux between samples. Capillary variations are key for efficient oxygen uptake by the fetus; they allow the blood to decelerate where the villous membrane is thinnest allowing for a better oxygenation, but also by reducing the vessel diameter they carry the oxygenated blood away fast. The methodology employed herein could become a platform to simulate complicated *in-vivo* and *in-vitro* scenarios of pregnancy complications.

Keywords: Blood Flow, Oxygen Transport, Terminal Villi, Placenta, Modeling

1. Introduction

The importance of placental blood circulation was already noted by Aristotle On the Generation of Animals, *ca* 340 B.C., due to its role in the transport of respiratory gases from the mother to her fetus. Because of the *in-vivo* ethical limitations and the complicated acquisition and manipulation of the *ex-vivo* organ, placental research has been very challenging. Furthermore, animal models are of limited use due to species differences in structure and biochemistry of the placenta (Battaglia and Meschia, 1986). As a consequence, the functional relationships between the maternal and fetal blood streams, at the level of the terminal villus (microscopic scale), are not well understood.

Maternal blood enters the placenta when it reaches the intervillous space via the uterine arteries, percolates between branches of the villous tree and returns deoxygenated to the maternal circulatory system through the uterine veins. On the other side, fetal blood flows from the umbilical arteries towards the branching trees of the chorionic vasculature, and oxygenated blood returns via the umbilical vein (Figure 1). The feto-placental capillaries are tortuous, have variable diameters and sharp bends (Plitman Mayo et al., 2016), making their architecture unique. The two circulations are brought into proximity in the villous tree, separated by the villous membrane. Placental gas exchange takes place at the terminal villi where vasculo-syncytial membranes form (Gill et al., 2011). These are localised areas where the membrane is thinnest, often as little as 1-2 μm (Burton and Tham, 1992).

*Corresponding author
Email address: mlo29@cam.ac.uk (M. L. Oyen)

Much attention has been given to the maternal placental circulation, *i.e.* uterine arteries and intervillous space blood flow (Serov et al., 2015, Chernyavsky et al., 2011, 2010, Sengupta et al., 1997, Heilmann et al., 1979), because maladaptations such as pre-eclampsia or intrauterine growth restriction (IUGR) are the source of pregnancy complications. The feto-placental circulation was almost neglected until Doppler ultrasound was proposed as an early risk assessment tool (Fitzgerald and Drumm, 1977). The easy and routine acquisition of *in-vivo* data provided the opportunity to investigate and validate various aspects of the fetal circulation, such as the haemodynamics of the umbilical cord (Bracero et al., 1989, Giles et al., 1986, Trudinger et al., 1985, Gill, 1979, Fitzgerald and Drumm, 1977), insights regarding the villous tree function and development (Guiot et al., 1992, Thompson and Stevens, 1989, Reuwer et al., 1986) and the understanding of the complete fetal circulatory system (Kiserud and Acharya, 2004, Fitzgerald et al., 1984). However, Doppler ultrasound cannot provide *in-vivo* information on the flow at the terminal vasculature due to limits of resolution. Histology has also failed to identify the flow regimes because the maternal and fetal blood streams are not arranged in parallel. Therefore, mathematical modeling has become the only accessible tool for providing insights regarding the microcirculation in human placental capillaries.

The flow in the terminal villi was initially modelled as a two-dimensional (2D) concurrent, countercurrent, cross-current or mixed (partly concurrent and partly countercurrent) system (Moll, 1971, Guilbeau et al., 1971, Bartels et al., 1962). There have been a few attempts to improve the placental microvasculature modeling, such as Reneau et al. (1974) who simulated the three-dimensional (3D) fetal capillary tissue as small cylinders inside a larger cylinder or Costa et al. (1992) who modelled whirling motion in the capillary bends (sinusoids) where blood mixing takes place. Although technological advances offer new modeling tools, computational simulations have been barely used in placental related research possibly due to the geometrical complexity (Reneau et al., 1974, Moll, 1971, Guilbeau et al., 1971, Bartels et al., 1962). Gordon et al. (2007) created a branching model of the chorionic arterial vasculature based on published data and solved the fetal blood flow field. However, the branching model does not reach the terminal villi and only includes a few intraplacental vessels. For a comprehensive review on the role of morphology in mathematical models of placental gas exchange, the reader is referred to Serov et al. (2016). To the best of the authors' knowledge, the circulation in feto-placental capillaries has not been satisfactorily simulated by either a mathematical or a computational model.

The main objective of this work was to better understand the structure-function relationship of human placental terminal villi. For that purpose, 3D blood flow simulations were performed in fetal capillaries reconstructed from confocal microscopic image stacks (Plitman Mayo et al., 2016, 2014). The impact of the variability in capillary diameter and tortuosity together with the blood flow direction and distribution on the oxygen transport was investigated and corroborated by an experimental validation.

2. Materials and Methods

2.1. Computational simulations

A fresh healthy placenta delivered by Cesarean section at term was obtained at the Department of Obstetrics & Gynaecology in Addenbrooke's Hospital, Cambridge (UK) for perfusion fixation, with ethical permission and informed written consent. Small tissue sample containing terminal villi were stained and scanned using a Leica SP2 CLSM (Leica Microsystems, Wetzlar, Germany) with an x25, 0.95NA objective lens.

Three-dimensional blood flow and oxygen transport was modeled in four terminal villi, reconstructed from microscopic image stacks (Plitman Mayo et al., 2016). Oxygen transport in the human placenta can be described as a six step process (Mayhew, 2014) in which (1) the oxygen dissociates from maternal red blood cells, (2) diffuses through maternal plasma, (3) diffuses across the trophoblastic epithelium, (4) diffuses across the basal lamina, villus stroma and endothelium, (5) diffuses through fetal plasma, and finally (6) binds to the haemoglobin of fetal erythrocytes. Herein, steps (1) and (2) are neglected since this work focuses on the feto-placental transport. Steps (3) and (4) differ in their diffusion coefficient values which should lead to different diffusion rates. However, due to the lack of information regarding these values, such steps are usually merged and referred to as 'diffusion across the villous membrane'. Steps (5) and (6) are assumed to be in equilibrium, taking place instantaneously. Therefore, in this study the computational models include the diffusion of oxygen across the villous membrane and through the fetal plasma.

Fick's second law of diffusion (Eq.1) has been widely used to model the transport of oxygen in placental villi due to the concentration ($\mathbf{C}$) gradients that arise between the outer surface of the villous membrane and the inner

surface of the fetal capillary endothelium (Serov et al., 2015, Mayhew, 2014, Gill et al., 2011). The maternal blood oxygen concentration (C_m) that surrounds the villous surface changes with time as a result of the maternal pulses from the uterine arteries, but also with the position (x, y, z) of the villi in the intervillous space. However, as a first approximation and due to the significant difference between the maternal blood travel time (~20 [s]) and the oxygen diffusion across a villus (order of seconds, Burton et al. (2009)), this concentration is assumed to be constant on the villi surface and the transport to be in a steady state ($\partial C/\partial t = 0$). Oxygen uptake by the villous membrane is neglected due to the lack of data; D_{vm} represents the diffusion coefficient of oxygen in the villous membrane.

$$D_{vm}(\frac{\partial^2 C}{\partial x^2} + \frac{\partial^2 C}{\partial y^2} + \frac{\partial^2 C}{\partial z^2}) = D_{vm}\nabla^2 C = 0 \tag{1}$$

Diffusion through the fetal plasma can be described as a combination of convective and diffusive transport. A linear combination of these two transport mechanisms results in the convection-diffusion equation (Eq.2). Here, D_b is the diffusion coefficient of oxygen in blood and $\mathbf{u}$ is the fluid velocity field. The initial oxygen concentration was assumed to be zero, representing deoxygenated fetal blood entering the villi; in this way the amount of oxygen leaving the capillaries can be easily quantified. A Neumann boundary condition was applied to the outlets such that the outflow is $-\mathbf{n} \cdot D_b \cdot \nabla C = 0$.

$$\nabla \cdot (D_b \nabla \mathbf{C}) - \nabla \cdot (\mathbf{u} \cdot \mathbf{C}) = 0 \tag{2}$$

The velocity field in the capillaries was found by solving the steady state Navier-Stokes equation (Eq.3) for a Newtonian incompressible fluid under laminar flow. Blood flow is known to be steady at the capillary level of the cardiovascular system (Bloor, 1968), therefore it was reasonable to assume the same in the fetal microvascular bed. The motion of discrete red blood cells was assumed to be that of a continous fluid. By assuming a Newtonian incompressible fluid, the effects of viscosity and density changes were ignored; both properties are unrelated to blood plasma but largely depend on the mechanical properties of red blood cells. Conservation of concentration and flux was ensured across the villous membrane.

Laminar flow can be assumed due to the small Reynolds number (0.001-0.0029, see Appendix A for details). Blood density was taken as $\rho = 1060$ [Kg/m^3] (Cutnell and Johnson, 1998) and blood's dynamic viscosity coefficient as $\mu = 3.5{\cdot}10^{-3}$ [Pa $\cdot$ s] (Bodnár et al., 2014). The fluid velocity was zero in the capillary walls (no-slip boundary), a zero pressure was defined in the outlets and a mean velocity, $\mathbf{u}$, was defined in the inlets. The mean velocity was applied at a distance far enough to allow for the flow to reach the terminal villi in a fully developed steady state. By setting the outlet pressure to zero the inlet pressure represents the pressure drop along the capillary. A schematic representation of the simulations is provided in Figure A.2.

$$\rho(\mathbf{u} \cdot \nabla)\mathbf{u} = \nabla \cdot [-p\mathbf{I} + \mu(\nabla \mathbf{u}) + (\nabla \mathbf{u})^T] + F \tag{3}$$

These three equations (Eqs. 1-3) were numerically solved by COMSOL Multiphysics 5.2, a finite element analysis commercial software. Tetrahedral meshes of 700,000-900,000 elements, depending on the model size and complexity, were automatically created by COMSOL. Since it is impossible to determine from microscopic images the real direction and distribution of the blood, all possible circulation scenarios within each specimen were solved and compared (Cugnoni et al., 2009). A schematic example of this analysis is given in Figure A.3.

A better way to understand the structure-function relationship in the terminal villi is by performing parametric studies of different model parameters. Table 1 provides details of these studies. The impact of the different values was assessed on the villous efficiency (Eq.4), calculated similarly to that previously reported (Plitman Mayo et al., 2016).

$$E = \frac{\text{Total Flux Magnitude}}{\text{Capillary Volume}} = \frac{\text{Diffusive Flux + Convective Flux Magnitudes}}{\text{Capillary Volume}} \tag{4}$$

2.2. Flow Validation

Due to scale constrains, a direct validation of the results is not doable. Therefore, to demonstrate the validity of the above equations a fluid visualization experiment was performed in a scaled plastic replica (by a factor of 10^3.). A subsection of specimen 2 (long U-protrusion) (Plitman Mayo et al., 2016) was selected for this comparison. A plastic

Table 1: Details of the parametric studies.

Variable	Parameter	Range
Maternal oxygen concentration	C_m [mol/m^3]	1 - 5
Oxygen diffusivity in blood[a]	D_b [m^2/s]	$1.2{\cdot}10^{-9}$ - $2.2{\cdot}10^{-9}$
Oxygen diffusivity the villous membrane[b]	D_{vm} [m^2/s]	$7.3{\cdot}10^{-10}$ - $2.2{\cdot}10^{-9}$
Inlet velocity[c]	u [mm/s]	0.1 - 1.5

[a] Hershey et al. (1967).
[b] Fischkoff and Vanderkooi (1975), Goldstick et al. (1976).
[c] Appendix A.

replica of the selected geometry was created by IPF (Industrial Plastic Fabrications Ltd, Nazeing, Waltham Abbey, UK) as shown in Figure A.4(a).

The capillary replica was filled with rapeseed oil and a near constant-flux flow was driven through the geometry by way of a peristaltic pump ($\approx$ 100 rotations per minute). An inflow velocity of 0.4082 [mm/s] was established, thus producing a Reynolds number 10^3 times higher than in the real geometries (order 1) and ensuring laminar flow.

In order to visualize the flow within the geometry, passive tracer particles (20 [μm] polyamide) with settling velocity much less than the advective velocity were added to the fluid reservoir. These particles have no observable effect on the motion of the fluid, but allow the observer to track the flow within the plastic replica. The geometry was back-illuminated using a LED array. A Dalsa (TELEDYNE Dalsa Inc, Waterloo, Canada), Falcon 2 camera was used to capture the progress of the particles through the geometry, recorded here at 25 frames per second.

The reconstruction of the flow field was done using Digiflow (Dalziel Research Partners, Cambridge, UK), a flow visualization software. Using a pattern matching algorithm between sequential pairs of images, the displacement of the fluid between frames can be calculated and the velocity field reconstructed. See Figure A.4(b) for a schematic of the methodology. By tracking the velocity field of the particles and applying a 5-point median filter to the data, the steady-state velocity field was reconstructed.

Computational simulations mimicking the experimental set-up were created. A laminar steady fluid flow was assumed and solved using the Navier-Stokes equation (Eq.3). The low concentration of passive tracer particles do not affect the rapeseed oil behaviour and therefore the material properties were assumed to be those of rapeseed oil: (μ = $7.88{\cdot}10^{-2}$ [Pa·s] and ρ = 907.3 [kg/m^3], Noureddini et al. (1992)). The results were extracted and compared with the experimental observations.

3. Results

3.1. Flow Validation

The simulated direction of the flow together with the experimental data is shown in Figure A.5(a) and A.5(b) respectively. Figure A.5(c) provides the speed of the flow along the center line of the geometry. There is an excellent agreement between the experimental data and the simulation results capturing the key features of the flow and the locations of peak velocities, except near the curvature (arclength, s = 110-130) where the experimental set-up begins to break down due to the flow normal to the image plane. Defects in the opacity of the geometry also contribute to some of the observed differences.

3.2. Computational simulations

The geometrical reconstructions showed that the fetal microvasculature is very complex with variable diameters, branches, loops and bends. The impact of these features is illustrated in Figure A.6. Figure A.6(a) shows the blood velocity in each terminal villus, Figure A.6(b) provides a magnification of a typical capillary segment and FigureA.6(c) plots the flow velocity along the centerline of the magnified segments (highlighted in blue in Figure A.6(b)). One may observe that the narrow segments transport the blood up to twice as fast as the dilated ones and that capillary bends (sinusoids) can decelerate the flow by up to 80%. Bifurcations are also shown to slow the blood's velocity. Additionally, it is demonstrated that no vortical flow can develop in the fetal capillaries since the fluid flow follows a

straight path rather than a rotational one. It is worth noting that the marked difference in specimen 1 velocity is due to a faster inlet flow rate.

The total oxygen flux, J, is plotted against the inlet flow rate in Figure A.7 for all the possible circulation scenarios of each specimen (Figure A.3). A strong correlation was found, indicating that a small rise in the flow rate greatly increases the total oxygen flux. The average oxygen flux in a terminal villus is $2.67 \cdot 10^{-16}$ [m·mol/s] with a $\pm 2.2 \cdot 10^{-16}$ [m·mol/s] standard deviation. Although most of the models fall within the standard deviation, the different scenarios within each specimen and the different architecture between samples led to significantly different results. This is best seen when comparing specimen 1 and 2; specimen 2 is able to transport the same amount of oxygen ($3 \cdot 10^{-16}$ [m·mol/s]) with half of the initial flow rate needed by specimen 1.

While the convective transport is mostly affected by the blood's velocity, the diffusive transport seems to be dictated by the overall distribution of the flow. This is best appreciated in Figure A.8, where the two fluxes - normalized by the inlet flow rate- are plotted along the centerline of the protruding U section of specimen 2 (marked in blue in Figure A.6(b)) in four representative circulation scenarios. Interestingly, the oxygen flux does not correlate with volume, surface area, villi to capillary volume or surface ratio.

The parametric studies suggest that the alteration of D_b or D_{vm} does not affect the overall efficiency, and that an increase of the velocity ultimately leads to a higher efficiency. The effect of the villous architecture remains unknown since the cross-sectional area varies along the fetal capillary and currently, there is no analytical description for this variability.

4. Discussion

This study combines 3D reconstructions from microscopic images with computational simulations to better model the transport function of the human placenta and to assess the structure-function relationship in the terminal villi. The data show that the variation in capillary diameter is key for effective oxygen uptake by the fetus (Figure A.6). The fetus invests the minimum energy needed for the blood to travel fast enough in order to provide oxygenated blood, but at the same time slow enough to allow for good oxygenation. This is achieved by a complex architecture where narrow and dilated segments are combined. The sinusoids reduce the diffusion distances, enabling a greater amount of oxygen to diffuse rapidly and better oxygenate the blood due to its deceleration. The narrow segments, which usually appear before and after a sinusoid, ensure a fast supply of deoxygenated blood and a fast removal of oxygenated blood. Kaufmann et al. (1985) suggested that the main functional importance of the capillary sinusoids is the reduction of vascular resistance; this work demonstrates that the capillary dilatations are crucial for an effective oxygen uptake. Therefore, their function is to promote a faster and better oxygenation while reducing the vascular resistance. The data also demonstrate that there is no vortical flow or whirling because that only develops in turbulent flows or as a result of geometrical spiralling.

Placental exchange can be dramatically increased by raising either the rate of extraction or by increasing the overall blood velocity (Reynolds et al., 2006). Since the diffusion coefficient of oxygen in blood is a material property that is unlikely to change significantly within the circulation within the circulation, it seems that increased blood velocity is the primary mechanism to increase exchange throughout pregnancy. Figure A.7 clearly shows this. The fact that most models fall within the standard deviation range suggests that the architecture of a terminal villus is such that a reverse flow does not dramatically affect the oxygen supply to the fetus.

The present work supports the statement made by Faber (1995) that it is not sufficient to know the magnitude of the fetal blood flow in the capillaries; the exact patterns and blood distribution between the villi must be known. Oxygen uptake is strongly influenced by the motion of fetal blood since it dictates the local changes of the oxygen concentration. Therefore, to accurately model gas transport in the terminal villi one should know the distribution of the fetal blood within the capillary network. This is clearly demonstrated in Figure A.8 where four different diffuse transport trends are found in the same geometry with different flow distributions. The fact that, after normalizing the values by the inlet flow rate, they still do not converge into a single line supports this statement. These results also support that the transfer of respiratory gases in the human placenta, such as oxygen, is almost entirely flow limited (Faber, 1995, Longo et al., 1971).

Oxygen consumption by the villous membrane and oxygen-hemoglobin binding were neglected to allow for the understanding of the blood flow impact in placental oxygen transport. Although oxygen-hemoglobin binding plays

a role in the transport of gases, it is the gradient of oxygen dissolved in the blood plasma and not the gradient of oxygen bound to haemoglobin that determines the rate of diffusion in blood (Metcalfe et al., 1967). The capillary wall elasticity was also neglected due to the lack of data regarding the material properties of the vessels. The elasticity of the fetal capillaries control the level of dilatation and may influence the blood motion. Lastly, the sample size is small but sufficient to provide proof of principle that the proposed technique works and provides useful insights.

One of the main reasons underlying the lack of studies regarding fetal blood flow and oxygen transport at the terminal villus scale is the difficulty of accurately describing the villus geometry. Modern engineering tools allow for the extraction and reconstruction of real terminal villus geometry from perfused placentae, which can thus be used as the basis of computational modeling. This study shows the advantages of combining immunofluorescent imaging and FEA for placental research, and demonstrates the capabilities of the technique previously proposed by the authors (Plitman Mayo et al., 2016) to become a powerful investigative tool. Additionally, this technology permits the investigation in detail of the structure-function relationship in the human placenta. It is expected that computational efforts will play a critical role in detecting possible pathologies and health risk for newborns in the future.

Conflict of Interest Statement

The authors confirm that there were no conflicts of interest associated with the funding or conduct of this work.

Acknowledgements

The first author gratefully acknowledges the generous support of Centre for Trophoblast Research, University of Cambridge, UK, which funded this work.

References

Bartels, H., Moll, W., Metcalfe, J., 1962. Physiology of Gas Exchange in the Human Placenta. Am J Obstet Gynecol 84, 1714–30.

Battaglia, F. C., Meschia, G., 1986. An Introduction to Fetal Physiology. Academic Press.

Benirschke, K., Burton, G. J., Baergen, R. N., 2012. Pathology of the Human Placenta. Springer.

Bloor, M. I. G., 1968. The Flow of Blood in the Capillaries. Phys. Med. Biol. 13, 443–450.

Bodnár, T., Galdi P., G., Nečasová, S., 2014. Fluid- Structure Iteraction and Biomedical Applications. Springer Basel.

Bracero, L. A., Beneck, D., Kirshenbaum, N., Peiffer, M., Stalter, P., Schulman, H., 1989. Doppler Velocimetry and Placental Disease. Am J Obstet Gynecol 161, 388–393.

Burton, G. J., Tham, S. W., 1992. The Formation of Vasculo-Syncytial Membranes in the Human Placenta. Journal of Developmental Physiology 18 (1), 43–47.

Burton, G. J., Woods, A. W., Jauniaux, E., Kingdom, J. C. P., 2009. Rheological and Physiological Consequences of Conversion of the Maternal Spiral Arteries for Uteroplacental Blood Flow during Human Pregnancy. Placenta 30 (6), 473–482.

Chernyavsky, I. L., Jensen, O. E., Leach, L., 2010. A Mathematical Model of Intervillous Blood Flow in the Human Placentome. Placenta 31 (1), 44 – 52.

Chernyavsky, I. L., Leach, L., Dryden, I. L., Jensen, O. E., 2011. Transport in the Placenta: Homogenizing Haemodynamics in a Disordered Medium. Phil. Trans. R. Soc A 369, 4162–4182.

Costa, A., Costantino, M. L., Fumero, R., 1992. Oxygen Exchange Mechanisms in the Human Placenta: Mathematical Modelling and Simulation. Journal of Biomedical Engineering 14, 385–389.

Cugnoni, J., Oyen, M. L., Charnock-Jones, D. S., Burton, G. J., 2009. Pressure-Regulated Gas Diffusion in Human Terminal Chorionic Villi. Reproductive Sciences 16, 284A.

Cutnell, J., Johnson, K., 1998. Physics *Fourth Edition*. Wiley.

Faber, J. J., 1995. Review of Flow Limited Transfer in the Placenta. International Journal of Obstetric Anesthesia 4, 230–237.

Fischkoff, S., Vanderkooi, J. M., 1975. Oxygen Diffusion in Biological and Artificial Membranes Determined by the Fluorochrome Pyrene. The Journal of General Physiology 65, 663–676.

Fitzgerald, D. E., Drumm, J. E., 1977. Non-invasive Measurement of Human Fetal Circulation Using Ultrasound: A New Method. British Medical Journal 2, 1450–1451.

Fitzgerald, D. E., Stuart, B., Drumm, J. E., Duignan, N. M., 1984. The Assessment of the Feto-Placental Circulation with Continuous Wave Doppler Ultrasound. Ultrasound in Med & Biol. 10, 371–376.

Giles, W. B., Lingman, G. r., Maršál, K., Trudinger, B. J., 1986. Fetal Volume Blood Flow and Umbilical Artery Flow Velocity Waveform Analysis: A Comparison. British Journal of Obstetrics and Gynaecology 93, 461–465.

Gill, J. S., Salafia, C. M., Grebenkov, D., Vvedensky, D. D., 12 2011. Modeling Oxygen Transport in Human Placental Terminal Villi. Journal of Theoretical Biology 291 (0), 33–41.

Gill, R. W., 1979. Pulsed Doppler with B-mode Imaging for Quantitative Blood Flow Measurement. Ultrasound in Med & Biol. 5, 223–235.

Goldstick, T. K., Ciuryla, V. T., Zuckerman, L., 1976. Diffusion of Oxygen in Plasma and Blood. Adv. Exp. Med. Biol. 75, 183–90.

Gordon, Z., Eytan, O., Jaffa, A., Elad, D., 2006. Hemodynamic Analysis of Hyrtl Anastomosis in Human Placenta. Am J Physiol Regul Integr Comp Physiol, R977–R982.
Gordon, Z., Eytan, O., Jaffa, A., Elad, D., 2007. Fetal Blood Flow in Branching Models of the Chorionic Arterial Vasculature. Annals of the New York Academy of Sciences, 250–265.
Guilbeau, E. J., Reneau, D. D., Knisely, M. H., 1971. The Effects of Placental Oxygen Consumption and the Contractions of Labor on Fetal Oxygen Supply. A Steady and Unsteady State Mathematical Simulation. Respiratory Gas Exchange and Blood Flow in the Placenta - Symposium Proceedings, 297–344.
Guiot, C., Pianta, P. G., Todros, T., 1992. Modelling the Feto-Placental Circulation: 1. A Distributed Network Predicting Umbilical Haemodynamics Throughout Pregnancy. Ultrasound in Med & Biol. 18, 535–544.
Heilmann, L., Grebner, H., Mattheck, C., H., L., 1979. Mathematical, Clinical, and Laboratory Study of Hemodynamic Changes in the Placental Circulation. Arch. Gynecol 227, 303–313.
Hershey, D., Miller, C. J., Menke, R. C., Hesselberth, J. F., 1967. Oxygen Diffusion Coefficients for Blood Flowing down a Weeted-wall Column. Chemical Engineering in Medicine and Biology, 117–134.
Kaufmann, P., Bruns, U., Leiser, R., Luckhardt, M., Winterhager, E., 1985. The fetal vascularisation of term human placental villi. ii. intermediate and terminal villi. Anatomy and Embryology 173 (2), 203–214.
Kiserud, T., Acharya, G., 2004. The Fetal Circulation. Prenatal Diagnosis 24, 1049–1059.
Longo, L. D., Hill, E. P., Power, G. G., 1971. Factors Affecting Placental Oxygen Transfer. Respiratory Gas Exchange and Blood Flow in the Placenta - Symposium Proceedings, 345–393.
Mayhew, T. M., 2014. Estimating Oxygen Diffusive Conductances of Gas-Exchange Systems: A Stereological Approach Illustrated with the Human Placenta. Annals of Anatomy 196(1), 34–40.
Metcalfe, J., Bartels, H., Moll, W., 1967. Gas Exchange in the Pregnant Uterus. Physiol. Rev. 47 (4), 782–838.
Moll, W., 1971. Gas Exchange in Countercurrent and Crosscurrent Flow Systems. The Concept of the Fetoplacental Unit. Respiratory Gas Exchange and Blood Flow in the Placenta - Symposium Proceedings, 281–294.
Noureddini, H., Tech, B. C., Davis Clements, L., 1992. Viscosities of Vegetable Oils and Fatty Acids. JAOCS 69, 1189–1191.
Plitman Mayo, R., Charnock-Jones, D. S., Burton, G. J., Oyen, M. L., 2016. Three-Dimensional Modeling of Human Placental Terminal Villi. Placenta 43, 54–60.
Plitman Mayo, R., Charnock-Jones, S. D., Burton, G. J., Oyen, M. L., 2014. 3D Surface Reconstruction of Human Terminal Villi and The Fetal Capillary Bed. Placenta 35, A8–A9.
Reneau, D. D., Guilbeau, E. J., Cameron, J. M., 1974. A Theoretical Analysis of the Dynamics of Oxygen Transport and Exchange in the Placental-Fetal System. Microvascular Research, 346–361.
Reuwer, P. J. H. M., Nuyen, W. C., Beijer, H. J. M., Heethaar, R. M., Haspels, A. A., Bruinse, H. W., 1986. Feto-Placental Circulatory Competence. Eur. J. Obstet. Gynecol. Reprod. Biol. 21, 15–26.
Reynolds, L. P., Caton, J. S., Redmer, D. A., Grazul-Bilska, A. T., Vonnahme, K. A., Borowicz, P. P., Luther, J. S., Wallace, J. M., Wu, G., Spencer, T. E., 2006. Evidence for Altered Blood Flow and Vascularity in Compromised Pregnancies. Journal of Physiology 1, 51–58.
Sengupta, A., Biswas, P., Jayaraman, G., Guha, S. K., 1997. Understanding utero-Placental Blood Flow in Normal and Hypertensive Pregnancy through a Mathematical Model. Med. Biol. Eng. Comput. 35, 223–230.
Serov, A. S., Salafia, C., Brownbill, P., Grebenkov, D. S., Filoche, M., 2015. Optimal Villi Density for Maximal Oxygen Uptake in the Human Placenta. Journal of Theoretical Biology 368, 133–144.
Serov, A. S., Salafia, C., Grebenkov, D. S., Filoche, M., 2016. The Role of Morphology in Mathematical Models of Placental Gas Exchange. Journal of Applied Physiology 120, 17–28.
Thompson, R. S., Stevens, R. J., 1989. Mathematical Model for Interpretation of Doppler Velocity Waveform Indices. Med. & Biol. Eng. & Comput. 27, 269–276.
Trudinger, B. J., Giles, W. B., Cook, C. M., Bombardieri, J., Collins, L., 1985. Fetal Umbilical Artery Flow Velocity Waveforms and Placental Resistance: Clinical Significance. British Journal of Obstetrics and Gynaecology 92, 23–30.

Appendix A. Laminar flow assumption

Reynolds number is commonly used to determine whether a specific flow can be assumed to be laminar, by relating the momentum forces (ρU) to the viscous forces (μ):

$$Re = \frac{\rho U D}{\mu} \tag{A.1}$$

where ρ is the density of the blood, U the mean velocity in the capillaries, D the mean diameter of the vessels and μ the dynamic viscosity.

Blood properties, ρ and μ, are taken from the literature (see Section 2.1) and the mean vessel diameter of the terminal villus ranges between 40-80 μm (Benirschke et al., 2012). The mean blood velocity in the fetal capillaries can be calculated from the total placental volume and blood's volumetric flow rate in the umbilical artery.

The mean volume of the villus tree is the product of the total placental volume ($V_{placenta}$ = 448[cm^3] (Benirschke et al., 2012)) and the percentage of villus volume per placenta (η = 57.9% (Benirschke et al., 2012)): $V_{villus} = V_{placenta} \cdot \eta$ = 259.4 [cm^3]. Because it is unknown whether the terminal villi are supplied by an intermediate villus or by a

neighbouring terminal villus, both cases are included herein. The fetal blood volume can therefore be defined as follows:

$$V_{blood} = V_{villus} \cdot \eta_1 \cdot \eta_2 \tag{A.2}$$

where η_1 is the volume of intermediate or terminal villus (27.8% and 38.7% respectively) and η_2 is the volume of vessels (21% and 45.2%) from the total villus volume (Benirschke et al., 2012). The mean velocity of the fetal blood in the terminal villi can be found from the ratio of the umbilical volumetric flow rate (Q = 500 [ml/min] (Gordon et al., 2006)) and the average cross sectional area of the capillaries ($S_{vessels} = V_{blood}/l_{villus}$):

$$U_{mean} = \frac{Q}{S_{vessels}} = \frac{Q \cdot l_{villus}}{V_{blood} \cdot \eta_1 \cdot \eta_1} \tag{A.3}$$

Equation A.3 results in U_{mean} = 0.275 [mm/s] for intermediate villus and U_{mean} = 0.735 [mm/s] for terminal villus. Therefore, the Reynolds number of the fetal blood flow ranges approximately between 0.0178-0.0033 and can be assumed to be laminar. This is in agreement with the previously reported values by Bloor et al. (Bloor, 1968).

List of Figures

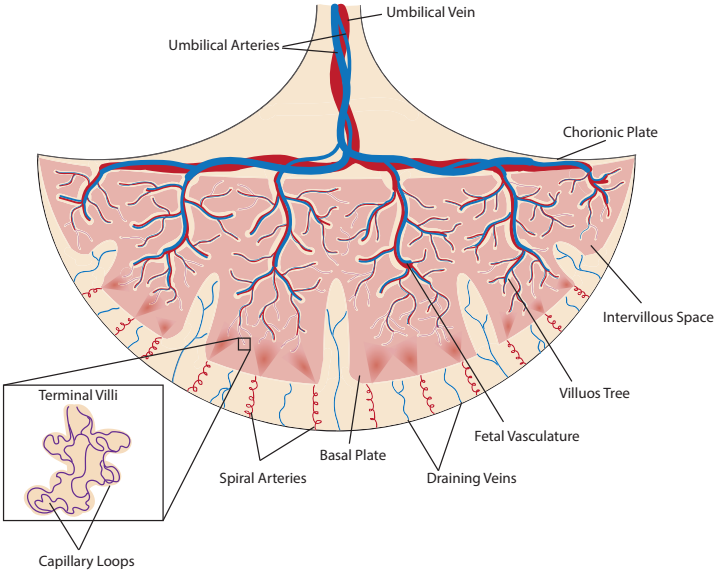

Figure A.1: Schematic representation of the human placenta showing its cross-section. Fetal blood perfuses the placenta from the umbilical arteries and returns oxygenated through the umbilical vein. Maternal blood reaches the placenta from the spiral arteries, percolates through the villous tree and returns deoxygenated through the draining veins.

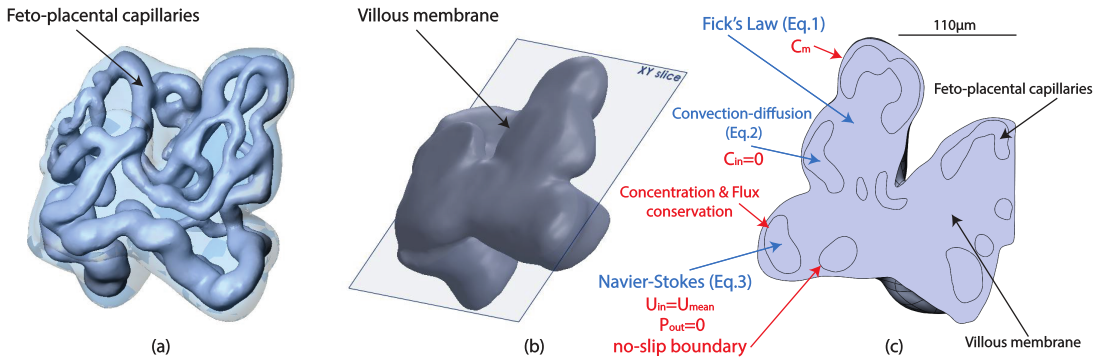

Figure A.2: Schematic representation of the numerical models. (a) the feto-placental capillaries domain, (b) the villous membrane domain and (c) a xy slice view outlining the equations (blue) and boundary conditions (red) for the computational simulations.

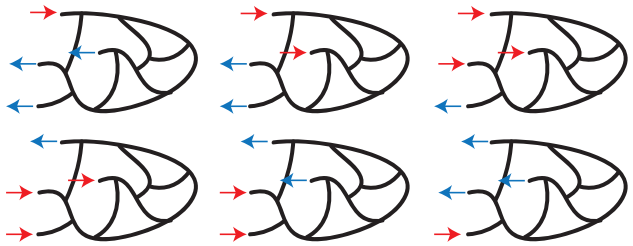

Figure A.3: Schematic representation of a terminal villus showing all the possible boundary conditions. Inlets are represented by red arrows and outlets as blue arrows. Each combination will lead to a different circulation scenario.

(a)

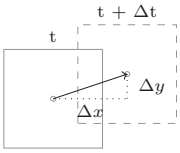

(b)

Figure A.4: (a) A scaled up (x1000) plastic replica of a capillary segment and (b) Schematic depiction of the velocity prediction algorithm; A window at time t is matched with the corresponding window at time $t + \Delta t$ then, the displacement between matching windows is used to reconstruct the velocity field.

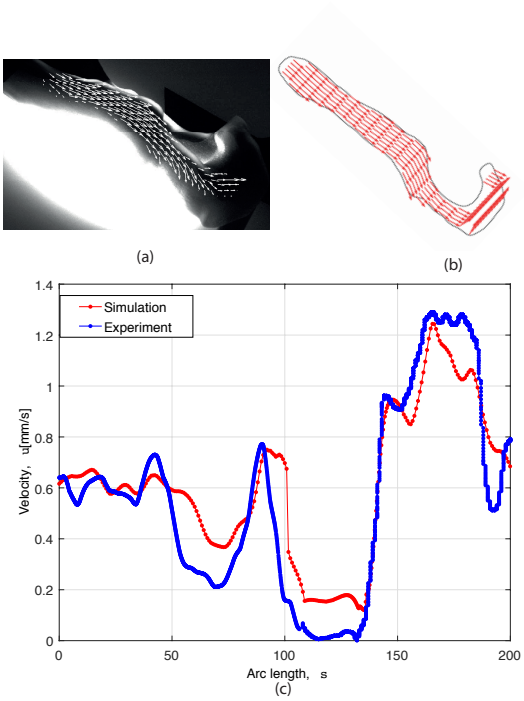

Figure A.5: Comparison of the experimental (a) and simulated (b) flow direction. (c) Experimental and simulated speed of flow along the center line of the geometry (mm/s).

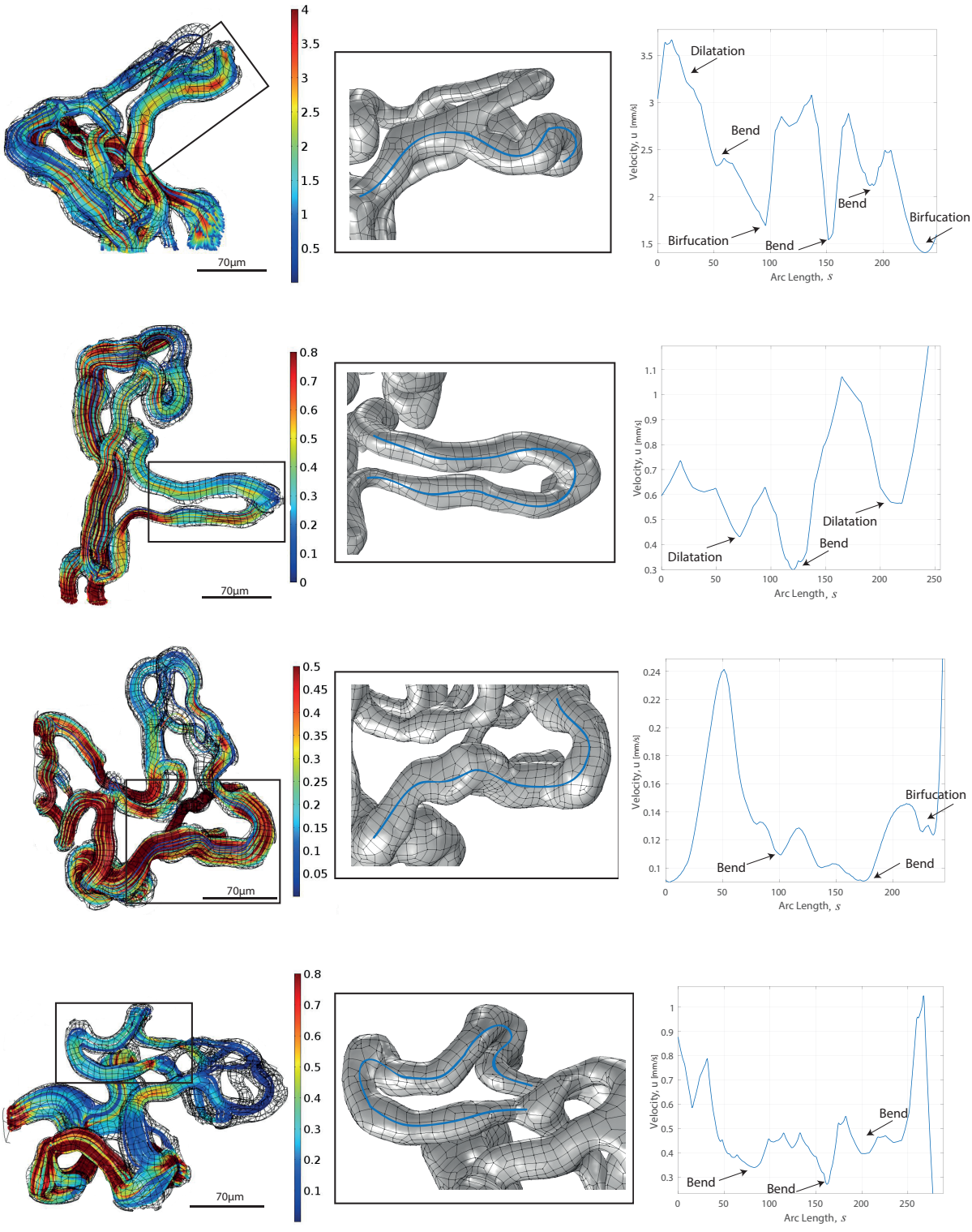

(a) (b) (c)

Figure A.6: (a) Blood velocity streamlines [mm/s] for all samples, (b) Magnification of typical feto-capillary segments with their respective center lines and (c) A velocity plot along the center lines of the magnified sections with key features highlighted.

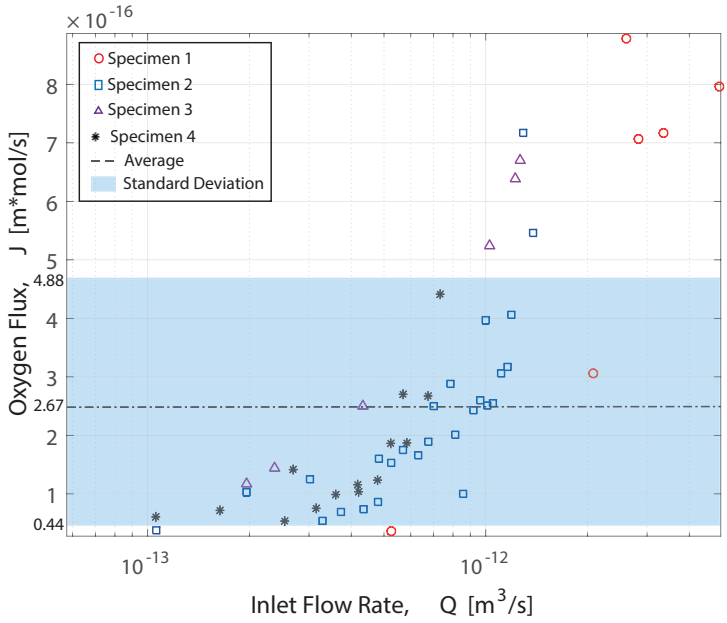

Figure A.7: Total oxygen flux vs. Inlet flow rate for all circulation scenarios of all specimens.

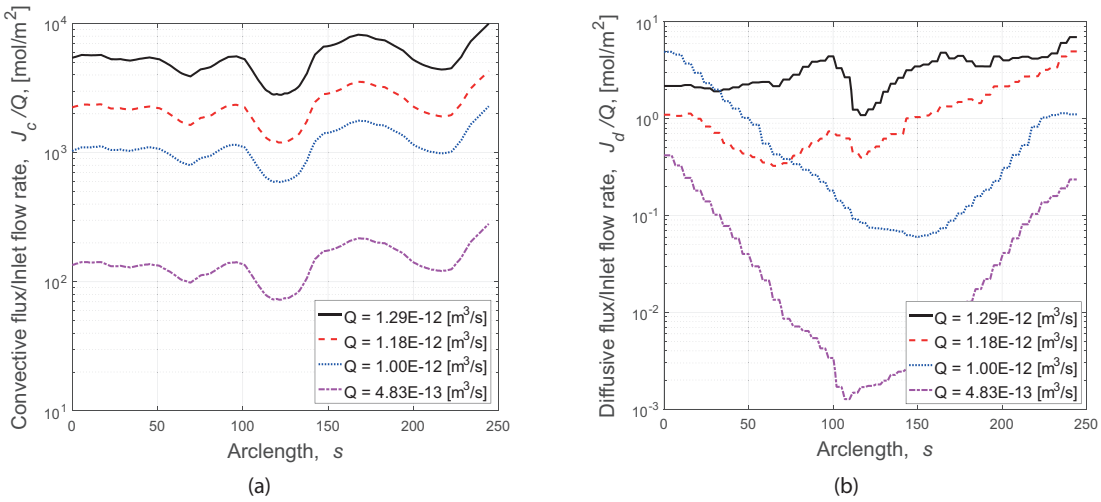

Figure A.8: (a) Convective transport and (b) Diffusive transport along the center line of the magnified section of specimen 2 (Figure A.6(b)).